# Myoelectric model-based control of a bi-lateral robotic ankle exoskeleton during even ground locomotion *

Guillaume Durandau, *Student Member, IEEE*, Wolfgang F. Rampeltshammer, Herman van der Kooij, *Member, IEEE*, and Massimo Sartori, *Member, IEEE*

***Abstract*— Individuals with neuromuscular injuries may fully benefit from wearable robots if a new class of wearable technologies is devised to assist complex movements seamlessly in everyday tasks. Among the most important tasks are locomotion activities. Current human-machine interfaces (HMI) are challenged in enabling assistance across wide ranges of locomoting tasks. Electromyography (EMG) and computational modelling can be used to establish an interface with the neuromuscular system. We propose an HMI based on EMG-driven musculoskeletal modelling that estimates biological joint torques in real-time and uses a percentage of these to dynamically control exoskeleton-generated torques in a task-independent manner, *i.e.* no need to classify locomotion modes. Proof of principle results on one subject showed that this approach could reduce EMGs during exoskeleton-assisted even ground locomotion compared to transparent mode (i.e. zero impedance). Importantly, results showed that a substantial portion of the biological ankle joint torque needed to walk was transferred from the human to the exoskeleton. That is, while the total human-exoskeleton ankle joint was always similar between assisted and zero-impedance modes, the ratio between exoskeleton-generated and human-generated torque varied substantially, with human-generated torques being dynamically compensated by the exoskeleton during assisted mode. This is a first step towards natural, continuous assistance in a large variety of movements.**

## I. Introduction

Human-exoskeleton interaction underlies a complex interplay between hardware, software and biological structures. Exoskeletons should enable navigation in complex unstructured environments *i.e.* home and outdoor environment (see Cybathlon competition [1]) to assist in everyday motor tasks. To achieve this, a direct neuro-mechanical link needs to be established between the exoskeleton and the human. Current human-machine interfaces (HMIs) rely on pre-generated joint position or torque profiles prescribed to the exoskeleton motors during at pre-determined gait phases [2] or online optimized joint torque patterns that minimize metabolic energy consumption [3]. However, these methods do not offer user's voluntary control over the exoskeleton and lack of adaptability to the external environment. Electromyograms (EMGs) have been incorporated into HMIs and combined with ground reaction force (GRF) data [4]. Other works incorporated EMGs in optimal controller objective functions [5] where assistance was modulated depending on EMG-exoskeleton synergies. However, these methods are designed for a specific and pre-defined locomotion mode and do not rapidly and dynamically adapt to locomotion mode changes. Moreover, these methods are bound to sensors that are not always fully wearable (e.g. GRF sensors) or use classification algorithms that need to be retrained for each new task. Furthermore, these methods do not provide information about the neuromusculoskeletal (NMS) states of the user, which can be valuable to provide personalized robotic assistance.

We recently proposed a subject-specific NMS model driven by EMG signals that can estimate human-generated muscles force and resulting joints torques in real-time [6] over a wide range of tasks (walking, calf rise, jump, backward walking and side stepping) and degrees of freedom (DOFs) with a single offline calibration step. We further extended this approach to control a multi-DOF exoskeleton [7], [8] to support post-stroke and incomplete spinal cord injury patients performing sited tasks.

In this paper, we further extend our HMI to support locomotion tasks by a model-based controlled bi-lateral ankle exoskeleton newly developed to assist healthy and SCI (i.e. Cybathlon competition). Our proposed HMI provides user's voluntary control of the exoskeleton. We conducted controlled experiments that show that the developed HMI can reduce EMG levels when compared to the minimal impedance modality (i.e. transparent mode). Importantly, results showed that across assisted and non-assisted conditions the total human-exoskeleton torque was approximately the same but the ratio between exo-generated and human-generated torque varied substantially, *i.e.* human-generated torques decreased during assisted conditions. This suggests that the user and the exoskeleton always successfully reached a mechanical equilibrium where locomoting became more economical for the human. We first present our HMI as well as the exoskeleton used to conduct the experiment and the low-level torque control. We then present the experimental protocol and the results.

## II. Method

### A. Bilateral ankle exoskeleton hardware and low-level control

For this study, we used the ankle module of the Symbitron exoskeleton [9], a full lower limb exoskeleton developed for paraplegic users, as a standalone ankle exoskeleton: Both ankles have two degrees of freedom, active plantarflexion and dorsiflexion as well as passive inversion and eversion, and weigh 4.56 kg each. Plantarflexion angle was measured with

* The study was partly supported by ERC Starting Grant INTERACT (803035) and the Netherlands Organization for Scientific Research (NWO), project no. 14429. The authors are with the Department of Biomechanical Engineering, Technical Medical Centre, University of Twente, Enschede 7522 NB, The Netherlands (e-mail: g.v.durandau@utwente.nl, m.sartori@utwente.nl).

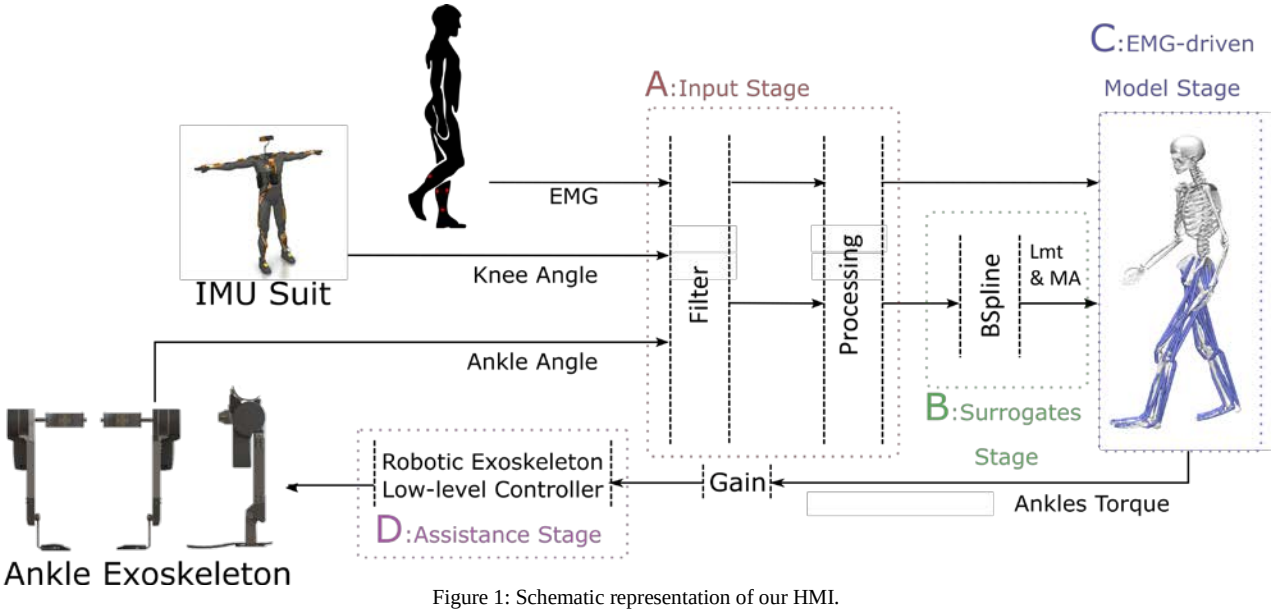


Figure 1: Schematic representation of our HMI.

absolute rotary encoders (AksIM, RLS, Renishaw, Slovenia). The ankles are actuated with custom Series Elastic Actuators (SEA) that can deliver a peak interaction torque of 100Nm. The interaction torque was computed from the spring deflection, which was measured with an absolute rotary encoder ( AksIM, RLS, Renishaw, Slovenia). The motor position was measured with an absolute angle hall encoder (MHM, IC Haus, Germany). The SEAs are controlled from a computer (NUC, Intel, USA) in the backpack that also contains the batteries and weighs 8kg. The controller is running in TwinCAT (Beckhoff, Germany) and communicates with the SEAs over Ethercat.

Each actuator controls for the interaction torque between user and exoskeleton using a controller specifically developed for the use in lower limb exoskeletons [10]. This torque controller achieves accurate torque tracking with a bandwidth of 30Hz as well as a low and passive apparent impedance. The low apparent impedance is equivalent to high transparency to user motions, while its passivity guarantees controller stability during impacts such as heel strike.

### *B. EMG-driven neuromusculoskeletal controller*

Our HMIs provides assistance based on joint torque computed by a real-time EMG-driven model previously developed [6], [8]. This torque is multiplied by a support ratio and sent to the exoskeleton. In Fig 1, we present a schematic of our HMI. It consists of the following stages:

1. **Input stage** (Fig. 1-A): the inputs of the controller are EMG and joint position. The EMG is directly provided by the exoskeleton to the controller via Ethercat (TwinCat, Beckhoff, Germany). The EMG envelop is computed by the electrodes (AxonMaster 13E500, Ottobock, Germany) and was normalized by the maximum voluntary contraction (MVC) of the user previously recorded. The ankle joint positions are provided also by the exoskeleton via Ethercat and the knees joint position are provided by an IMU suit (MVN Link, Xsens Technologies B.V, The Netherlands) via TCP/IP.
2. **Moment arm (MA) and muscle tendon length (LMT) surrogates stage** (Fig. 1-B): The joint position is transformed into muscle MA and LMT using a Bspline algorithm [11]. The Bspline coefficients are computed using a scaled model of the user and the OpenSim [12] muscle analysis tool.
3. **EMG-driven model stage** (Fig. 1-C): The LMT and EMG of the tibialis anterior, soleus, gastrocnemius (lateral and medial) from the left and right leg are transformed into muscle force with a Hill type muscle model using the following equation:
   Eq.1 $F^{MTU}(t) = F^{T} = F^{Max}\big(f(L^{M})f(V^{M})E(t) + f_{p}(L^{M})\big)\cos(\alpha^{M}(t))$
   With $F^{MTU}(t)$ the MTU force at instant t, $F^{T}$ the tendon force, $F^{Max}$ the maximal isometric force, $f(L^{M})$ the force-length relationship, $f(V^{M})$ the force-velocity relationship, $E(t)$ the normalized muscle activation at instant t. $f_{p}(L^{M})$ is the passive force length relationship and $\alpha^{M}(t)$ the pennation angle. More information can be found in [13].The muscle force is then projected at the joint to compute joint torque using MA.
4. **Assistance stage** (Fig. 1-D): The right and left ankle torque computed in real-time by the EMG-driven HMI are multiplied by a gain selected by the user. The assistance is then send to the low-level torque controller via Ethercat.

### *C. Personalization of the model for subject specific assistance*

To offer natural and task independent assistance, the NMS model needs to be personalized at multiple level. We first scale an OpenSim model using the scaling tool so that the standard model [14] fits the anthropomorphic subject proportion (bodies length, inertia and mass). For this, markers data of a static trial recorded from a motion capture system are used

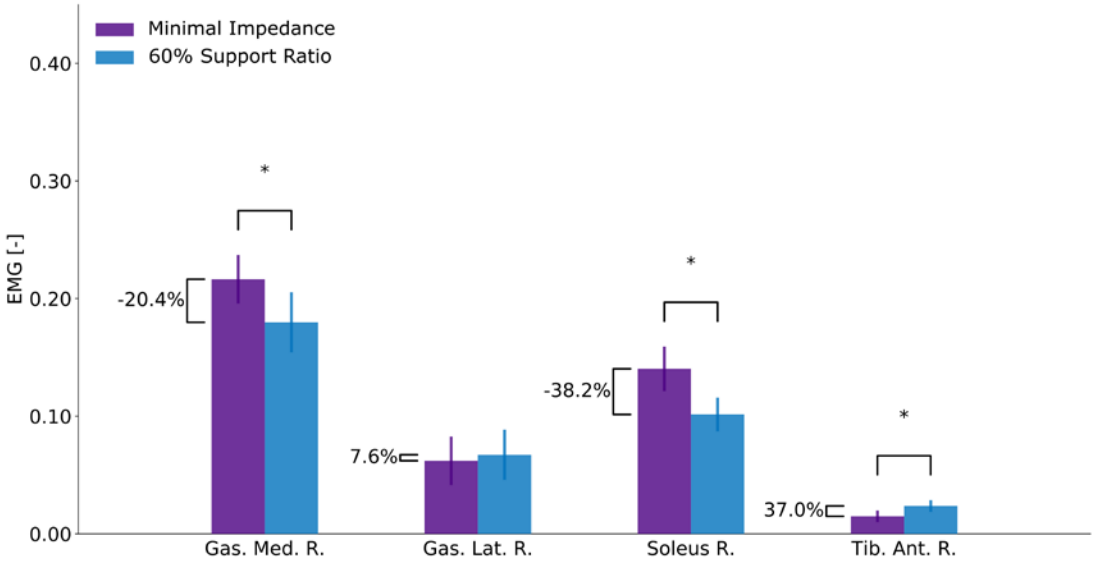


Figure 2: EMG reduction between the two tested conditions (minimal impedance mode (purple) and 60 % support ratio (blue)). Results are reported for the four recorded muscle on the right side. The bar represents the mean of all gait and the stick the standard deviation. * represents significance (P < 0.05).

(Qualisys Oqus, Qualisys AB, Sweden). We then use a pre-tuning algorithm to precompute optimal fiber length and tendon slack length for each considerate muscles [15]. We finally calibrate optimal fiber length, tendon slack length, maximal muscle forces and activation shape factor using an optimization procedure based on the simulated annealing algorithm. The objective function consists of reducing the error between experimental joints torque computed by the inverse dynamic tool from OpenSim and the joints torque computed by the EMG-driven model. The experimental joint torque is computed from joint position from the inverse kinematic tool from OpemSim and ground reaction forces (GRF) recorded by an instrumentalized treadmill (M-Gait, MotekForce Link, The Netherlands).

### *D. Data processing*

Gait cycles were automatically segmented via a peak detection algorithm on the knee joint angle. The root mean squared (RMS) value for each gait cycle of each muscles' EMG, joints torque computed from our HMI and interaction torques (assistance given by the exoskeleton) were computed. Abnormal values were then removed if there were superior to three time the interquartile value. Finally, percentage of change between conditions (assistance and minimal impedance) was calculated as well as the t-test (t-test function from the python scipy library).

## III. EXPERIMENTS

### *A. Experimental protocol*

One healthy subject (age 38, mass 72 kg, height 180 cm) was recruited for this experimentation, which was based on a three-day protocol. The first day consisted on recording data for the personalization of the NMS model. Marker data, GRF data and EMG data were recorded at 128 Hz, 2048 Hz and 2048 Hz respectively during different tasks. The tasks consisted of one static pose at the beginning and the end of the recording, MVC, calf rise, toe rise and walking at a speed of 1.8 km/h and 2.8 km/h without the exoskeleton. The recorded data were processed using MotoNMS [16] Matlab (Matlab 2016B, MathWorks, USA) scripts.

The data were then used for scaling and calibrating the NMS model as explained in the Methods Section. The second day consisted of a preparation and testing session. In this session, we first let the subject wore the exoskeleton and walked on a treadmill (Thera-Treadpro, Sportplus) with the exoskeleton in minimal impedance mode. This was done with the purpose of letting the user get used to the exoskeleton's added weight and inertia. The minimal impedance mode is a transparent mode where the exoskeleton's controller minimizes the interaction torque between the user and the exoskeleton. When the user

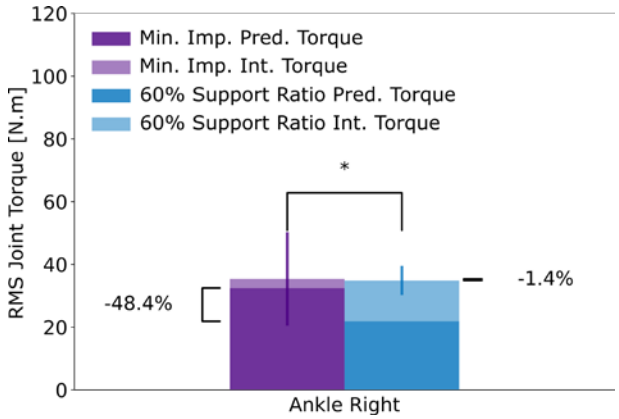


Figure 3: Torque reduction between the two tested conditions (minimal impedance mode (purple) and 60 % support ratio (blue)) and in dark the predicted joint torque form the model and in light the recorded interaction joint torque. Results are reported for the right ankle plantar-dorsiflexion joint. The bar represents the root mean squared of all gait and the stick the standard deviation. * represents significance (P < 0.05)

would feel comfortable and the user's gait looked natural, we would then run our HMI in real-time and in open-loop (without providing assistance). We then would visually inspect the torque profile of the predicted torque using the graphical user interface (GUI) of our HMI. If the torque prediction quality was judged good (similar to literature gait torques profile), we would then close the loop and provide assistance to the user. As our subject was a naïve user of exoskeleton, we started with low assistance (20 % of the joint torque back to the user) and slowly increase the assistance to a maximum of 60% support ratio. The last day consisted of the recordings. The trial consisted of one task of 3 minutes of walking at 1.8 km/h without any inclination. The task was repeated for each condition with 10 min rest in between. The tested condition are minimal impedance and 60% assistance from our HMI. The participant was asked to follow the rhythm of a metronomes to control for step length (found during day 2). During all experiments where the user had to walk with the exoskeleton a fall prevention device (ZeroG, Aretech LLC, USA) was used which give a body weight support of 5 Kg.

## IV. Results

### A. EMG reduction

In Fig. 2, we present the EMG reduction between the two conditions tested, minimal impedance and assistance from our HMI. We can see in Fig. 2, that we obtained a reduction in EMG level for the gastrocnemius medial (20.4% (significant)) and the soleus (38.2% (significant)). The gastrocnemius lateral underwent an increase of 7.6% (not significant) as well as the tibias anterior (37% (significant)).

### B. Torque reduction

In Fig. 3, we show the overall reduction in predicted joint torque as well as the added joint torque given by the exoskeleton's assistance (recorded interaction torque). The predicted joint torque about ankle plantar-dorsiflexion DOF was reduced by 48.4% (significant) between minimal impedance and assisted condition. When the interaction torque recorded by the exoskeleton was added to the predicted joint torque the overall torque is identical (difference of only 1.4%).

## V. Discussion

We proposed a model-based human-exoskeleton interface that reduced the human-generated EMG and ankle joint torques needed to locomote. Fig. 3 shows that total human-exoskeleton ankle joint torque, with and without assistance are approximately the same. This demonstrates that the exoskeleton assistance is directly integrated by the user, thereby lowering biological joint torque levels by the same amount as the received torque from the exoskeleton. This demonstrates that a force generation transfer was established from the human to the exoskeleton, thereby underlying a symbiotic relation between the human and the exoskeleton mediated by our proposed HMI. This also highlights the natural aspect of our HMI as otherwise the overall joint torque (user's own torque plus assistance) would be different than the one without assistance, i.e. due to possible additional torque required by the user to counteract for ill-timed assistance.

Results showed that 60% support ratio levels resulted in a 48% reduction of the predicted joint torque during locomotion. In this, 12% of the assistance is lost, which can be due to misalignment, sensor error/noise or fat tissue. Future work will investigate how to maximize force transfer between the exoskeleton and the user.

Fig. 2 shows that the provided assistance offered a reduction in EMG for the soleus and gastrocnemius medial, the gastrocnemius lateral had a small increase, which was not significant. The tibialis anterior underwent a small increase during the swing phase, which was due to off-ground ankle joint instability. This instability may result from the low stiffness of the user during swing, which allows for small angular oscillations when exposed to external force (i.e. the provided assistance). Future work will investigate the difference in EMG reduction across muscles and reduce the instability during swing phase assistance via joint stiffness estimation [17], i.e. with an assistance changing depending on how stiff the joint is.

We previously demonstrated that our HMI can extrapolate outside of the calibration data [6]. In [8], we showed that we can give assistance during sited tasks using only a model calibrated with isometrics contraction. For walking, which is a more complex task, we could not use such simple calibration successfully during this pilot. This can maybe due to the muscle working in a more dynamic range as well as by the added weight (4.5 Kg on each leg and 10 Kg for the backpack) and inertia to the leg. That is why we used walking tasks without wearing the exoskeleton for calibration. Further research will be conducted to determine the minimal calibration dataset that can be used for robustly controlling an exoskeleton.

Our proposed HMI relies on EMG signal detection to be reliable, i.e. free of movement artefact or disconnection. This required to integrate EMG sensors tightly with the exoskeleton. Future work will employ predicting modelling for reducing dependency on bio-electrical sensors. This experiment was a proof of concept for our HMI. We will conduct further experiments on more subjects and more walking tasks (different speed and inclination).

## VI. Conclusion

We presented a new HMI based on EMG-driven musculoskeletal modelling that enabled user's voluntary control of a bi-lateral ankle exoskeleton during locomotion. Results indicated assistive torques being transferred to the human that made locomotion more economical for the user, *i.e.* with EMG and biological torque reduction. These results could open new opportunities for enabling exoskeleton voluntary control in both industry and rehabilitation scenarios.

## References


[1] R. Riener, "The Cybathlon promotes the development of assistive technology for people with physical disabilities," *J. Neuroeng. Rehabil.*, vol. 13, no. 1, p. 49, 2016.

[2] A. T. Asbeck, S. M. M. De Rossi, K. G. Holt, and C. J. Walsh, "A

biologically inspired soft exosuit for walking assistance," *Int. J. Rob. Res.*, vol. 34, no. 6, pp. 744–762, 2015.

[3] J. Zhang *et al.*, "Human-in-the-loop optimization of exoskeleton assistance during walking," *Science (80-. ).*, vol. 356, no. 6344, pp. 1280–1283, 2017.

[4] K. Z. Takahashi, M. D. Lewek, and G. S. Sawicki, "A neuromechanics-based powered ankle exoskeleton to assist walking post-stroke : a feasibility study," pp. 1–13, 2015.

[5] R. W. Jackson and S. H. Collins, "Heuristic-Based Ankle Exoskeleton Control for Co-Adaptive Assistance of Human locomotion," *IEEE Trans. Neural Syst. Rehabil. Eng.*, vol. PP, no. c, pp. 1–10, 2019.

[6] G. Durandau, D. Farina, and M. Sartori, "Robust Real-Time Musculoskeletal Modeling driven by Electromyograms," *IEEE Trans. Biomed. Eng.*, 2017.

[7] N. Lotti *et al.*, "Adaptive model-based myoelectric control for a soft wearable arm exosuit: A new generation of wearable robot control," *IEEE Robot. Autom. Mag.*, p. 0, 2020.

[8] G. Durandau *et al.*, "Voluntary control of wearable robotic exoskeletons by patients with paresis via neuromechanical modeling," *J. Neuroeng. Rehabil.*, vol. 16, no. 1, p. 91, 2019.

[9] C. Meijneke, S. Wang, V. Sluiter, and H. van der Kooij, "Introducing a modular, personalized exoskeleton for ankle and knee support of individuals with a spinal cord injury," in *Wearable robotics: challenges and trends*, Springer, 2017, pp. 169–173.

[10] H. van der K. W.F. Rampeltshammer, A.Q.L. Keemink, "An improved force controller with low and passive apparent impedance for series elastic actuators," *IEEE/ASME Trans. on Mechatronics*.

[11] M. Sartori, M. Reggiani, A. J. van den Bogert, and D. G. Lloyd, "Estimation of musculotendon kinematics in large musculoskeletal models using multidimensional B-splines," *J. Biomech.*, vol. 45, no. 3, pp. 595–601, 2012.

[12] S. L. Delp *et al.*, "OpenSim: open-source software to create and analyze dynamic simulations of movement," *Biomed. Eng. IEEE Trans.*, vol. 54, no. 11, pp. 1940–1950, 2007.

[13] F. E. Zajac, "Muscle and tendon: properties, models, scaling, and application to biomechanics and motor control.," *Critical reviews in biomedical engineering*. 1989.

[14] S. L. Delp, J. P. Loan, M. G. Hoy, F. E. Zajac, E. L. Topp, and J. M. Rosen, "An interactive graphics-based model of the lower extremity to study orthopaedic surgical procedures," *IEEE Trans. Biomed. Eng.*, vol. 37, no. 8, pp. 757–767, 1990.

[15] C. R. Winby, D. G. Lloyd, and T. B. Kirk, "Evaluation of different analytical methods for subject-specific scaling of musculotendon parameters," *J. Biomech.*, vol. 41, no. 8, pp. 1682–1688, 2008.

[16] A. Mantoan, C. Pizzolato, M. Sartori, Z. Sawacha, C. Cobelli, and M. Reggiani, "MOtoNMS: A MATLAB toolbox to process motion data for neuromusculoskeletal modeling and simulation," *Source Code Biol. Med.*, vol. 10, no. 1, p. 1, 2015.

[17] M. Sartori, M. Maculan, C. Pizzolato, M. Reggiani, and D. Farina, "Modeling and simulating the neuromuscular mechanisms regulating ankle and knee joint stiffness during human locomotion," *J. Neurophysiol.*, vol. 114, no. 4, pp. 2509–2527, 2015.